AGU100 ADVANCING EARTH AND SPACE SCIENCE

Geophysical Research Letters

RESEARCH LETTER
10.1029/2018GL078407

Key Points:
- We present the first observational evidence of a direct connection between Mercury's exosphere and the surface crustal composition
- A 1:1 correlation was found between the production of magnesium and the regional distribution of magnesium on Mercury's surface
- Our results support theoretical arguments that micrometeoroid impact vaporization can directly source material from the regolith of rocky, airless bodies

Supporting Information:
- Supporting Information S1

Correspondence to:
A. W. Merkel,
aimee.merkel@lasp.colorado.edu

Citation:
Merkel, A. W., Vervack, R. J., Jr., Killen, R. M., Cassidy, T. A., McClintock, W. E., Nittler, L. R., & Burger, M. H. (2018). Evidence connecting Mercury's magnesium exosphere to its magnesium-rich surface terrane. *Geophysical Research Letters, 45*. https://doi.org/10.1029/2018GL078407

Received 17 APR 2018
Accepted 19 JUN 2018
Accepted article online 26 JUN 2018

Evidence Connecting Mercury's Magnesium Exosphere to Its Magnesium-Rich Surface Terrane

Aimee W. Merkel[1], Ronald J. Vervack Jr.[2], Rosemary M. Killen[3], Timothy A. Cassidy[1], William E. McClintock[1], Larry R. Nittler[4], and Matthew H. Burger[5]

[1]Laboratory for Atmospheric and Space Physics, University of Colorado Boulder, Boulder, CO, USA, [2]Johns Hopkins Applied Physics Laboratory, Laurel, MD, USA, [3]Solar System Exploration Division, NASA Goddard Space Flight Center, Greenbelt, MD, USA, [4]Department of Terrestrial Magnetism, Carnegie Institution of Washington, Washington, DC, USA, [5]Space Telescope Science Institute, Baltimore, MD, USA

Abstract Mercury is surrounded by a tenuous, collisionless exosphere where the surface of the planet is directly exposed to the space environment. As a consequence, impacts and space weathering processes are expected to eject atoms and molecules from the surface into the exosphere, implying a direct link between the exospheric composition and the planet's regolith material. However, observational evidence demonstrating this link has been elusive. Here we report that exospheric magnesium, a species recently discovered and systematically measured by the Mercury Surface, Space ENvironment, GEochemistry, and Ranging mission, is enhanced when observed over a portion of the planet's surface regolith rich in magnesium. These observations confirm a direct link between Mercury's magnesium exosphere and the underlying crustal surface composition, providing strong evidence supporting theoretical arguments that impact vaporization can directly supply material to the exosphere from the regolith of a rocky, airless body.

Plain Language Summary Understanding the physical processes that release atoms and molecules from Mercury's surface into its exosphere (highly tenuous atmosphere) has been a major challenge because it is difficult to observe Mercury from the ground or Earth's orbit. From its orbit around the planet, the Mercury Surface, Space ENvironment, GEochemistry, and Ranging mission provided the first detailed view of Mercury's surface composition and its space environment. Because Mercury is an airless body, its exosphere must constantly be replenished, and it has been assumed that it is directly sourced from the planet's surface. However, a direct observation connecting the surface and the exosphere was not possible until the Mercury Surface, Space ENvironment, GEochemistry, and Ranging mission. Using observations of exospheric magnesium (Mg) and colocating them with a Mg-rich region of Mercury's surface shows for the first time that such a link exists. The results suggest that incoming micrometeoroid particles (dust) can access the surface crustal composition directly and release Mg atoms into the surrounding environment. Our work will inform future exospheric models and provide insights into airless body processes for both other solar system objects and Mercury-like exoplanets.

1. Introduction

Of the terrestrial planets, only Mercury lacks a classical, collision-dominated atmosphere. Instead, the innermost planet is surrounded by an exosphere consisting of a tenuous collection of atoms and molecules that are more likely to be lost to space or collide with the surface than with each other. Because Mercury is an airless body, surface interactions with interplanetary dust, micrometeoroids, solar ultraviolet radiation, and solar wind particles are thought to directly access the surface regolith and eject atoms and molecules from it into the exosphere (Killen et al., 2007; Raines et al., 2015). Although it is generally assumed that the bulk of the exosphere is sourced from the planet's surface, observations directly connecting the distribution of exospheric density to variations in the regional surface composition have been lacking.

Before the Mercury Surface, Space ENvironment, GEochemistry, and Ranging (MESSENGER mission), analysis of Earth-based observations of exospheric sodium (Na), the species most routinely observed with ground-based telescopes, provided our greatest insight into the source mechanisms that supply Mercury's exosphere. Many researchers interpreted the spatial and temporal distribution of ground-based measurements of exospheric Na to infer its source (s). Because the spatial and temporal distribution of an exospheric species is influenced by a number of parameters and processes, including ejection energy, gravity, radiation pressure,

and photoionization with subsequent electric field transport, it was difficult to correlate the Na observations with the regional surface composition. Furthermore, the compositional distribution of Mercury's crust was not known before MESSENGER; therefore, model estimates of exospheric production routinely assumed that Mercury's surface was composed of a constant, globally uniform distribution of neutral-bearing minerals, making it difficult to isolate a direct connection between the surface and the exosphere (Burger et al., 2010; Sarantos et al., 2011; Schmidt, 2013).

Without direct observational evidence, many researchers theorized that Mercury's sodium exosphere might not reflect the underlying surface composition (Killen et al., 2010; Leblanc & Johnson, 2010; Morgan et al., 1988; Potter et al., 2002; Sprague et al., 1990; Wurz et al., 2010). Because Na is a volatile, Leblanc and Johnson (2010) in particular concluded from model simulations that the bulk of the observed Na exosphere is sourced from recycled and redistributed surface-adsorbed atoms that create a veneer of Na atoms on the exterior of Mercury's regolith (called the surface reservoir). To explain the Na observations, they postulated that impact vaporization initially released sodium atoms from the regolith into the exosphere with subsequent redistribution to create a uniform veneer of lightly bound Na atoms that are then recycled through low-energy processes such as thermal vaporization. Therefore, the production of exospheric Na is closely tied to this surface reservoir, which is a function of Mercury's true anomaly angle and not related to the underlying regolith itself, thus masking any direct connections between Na and the surface composition. Additionally, the low spatial resolution available in ground-based observations severely limits detection of small-scale regional variations in density.

Other species were also observed from Earth before MESSENGER, primarily potassium (K; Potter & Morgan, 1986) and calcium (Ca; Bida et al., 2000; Domingue et al., 2007; Killen et al., 2007, and references therein). Calcium in particular has been shown to have a large-scale height (Killen et al., 2005), and impact vaporization has been theorized as the dominant release process, indicating that direct connections to the surface might be observable. Owing to the difficulty in making these measurements from Earth, however, both K and Ca have been observed much more infrequently than Na and have provided little in the way of spatial or temporal information, so a direct connection to the surface composition could not be established.

Prior to the MESSENGER mission, the existence of any direct connections between the exospheric density distribution and the regional surface composition was thus difficult to establish. In addition, the ability of specific release processes, particularly impact vaporization, to directly access the surface regolith and release *new* atoms into the exosphere could not be confirmed. MESSENGER observations now provide a means to search for these direct connections and investigate the release processes more thoroughly through a direct comparison of exospheric observations from the Ultraviolet and Visible Spectrometer (UVVS) channel of the Mercury Atmospheric and Surface Composition Spectrometer (MASCS) instrument (McClintock & Lankton, 2007) to elemental surface composition maps derived from the X-ray spectrometer (XRS) observations (Schlemm II et al., 2007). These observations show for the first time that a direct link between the surface regolith and the exosphere does, in fact, exist.

2. Observations, Analysis, and Results

New elemental composition maps derived from XRS data show that Mercury's surface composition is not as uniform as previously assumed (Nittler et al., 2016; Weider et al., 2015). In particular, the XRS magnesium-to-silicon (Mg/Si) ratio map revealed a large geochemically concentrated terrane between 240°E and 320°E longitude in the mid-Northern Hemisphere that is rich in magnesium (Nittler et al., 2016; Weider et al., 2015). Figure 1b shows the surface Mg/Si ratio that has a large dynamic range with an abundance within the Mg-rich terrane boundary that can be more than 5 times higher than the surrounding terrane. This revelation motivated our search to determine if the Mg contained within the surface regolith is an important direct source of Mg in the exosphere.

The UVVS on MESSENGER made the first detections of Mg in Mercury's exosphere during MESSENGER's second flyby of Mercury on 6 October 2008 (McClintock et al., 2009). While in orbit about Mercury, the UVVS made near-daily measurements of exospheric Mg emission above Mercury's equatorial limb over ~4 Earth years. The near-daily observations taken during the orbital phase of the mission provided an extensive data set that enabled the first thorough characterization of the dayside temporal and spatial distribution of exospheric Mg (Merkel et al., 2017). Merkel et al. (2017) demonstrated that the variation in Mg emission is

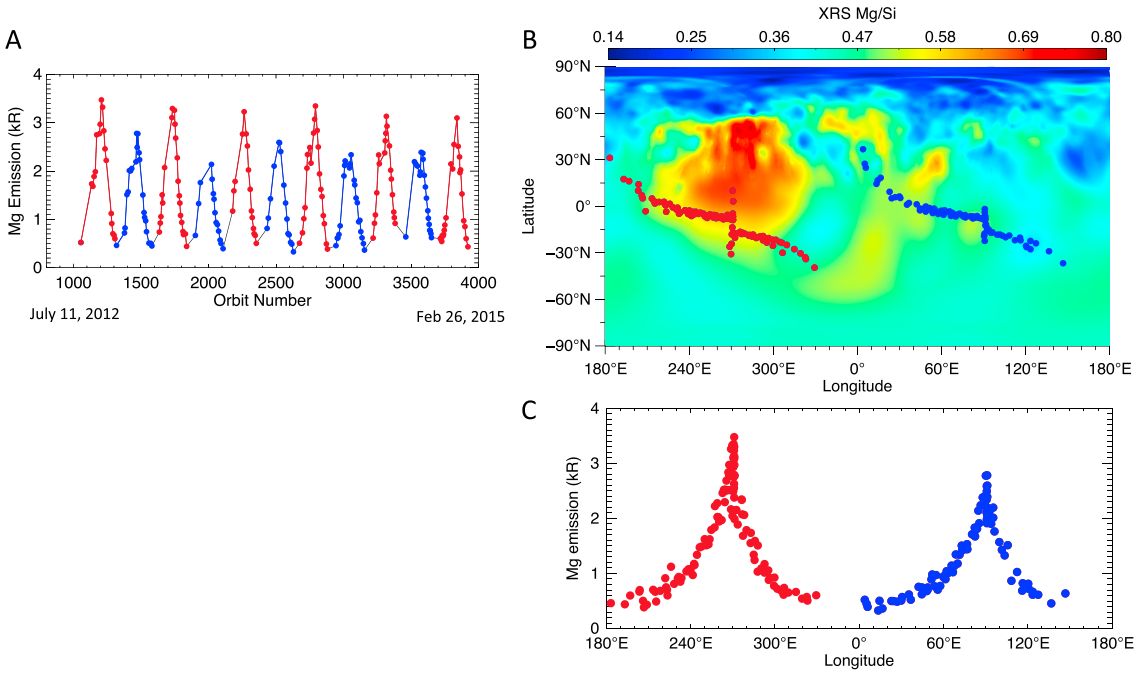

Figure 1. (a) Time series of Mg emission (measured in kiloRayleigh, where 1 kiloRayleigh is 10^9 photons emitted into 4π stradians in 1 second) observed at 300-km tangent altitude near the dawn terminator. The red and blue symbols highlight every other Mercury year. (b) Mg/Si elemental weight ratio composite map derived from XRS measurements. The red and blue circles represent the location of the Mg emission observations in (a). (C) Mg emission from (a) plotted with respect to longitude maintaining the red and blue color coding to indicate the location of every other year. XRS = X-ray spectrometer.

highly seasonally dependent with a predominant enhancement in emission, and thus production, in the morning near perihelion (Figure S2 in the supporting information). They identified micrometeoroid impact vaporization as the most likely dominant source process supplying the exosphere with Mg based on the observed temperatures, though the magnitudes and variations in temperature suggest that the Mg could be released directly and/or through the dissociation of a molecule released during the impact (Berezhnoy, 2018; Killen, 2016; Leblanc & Johnson, 2010; Valiev et al., 2017). With an impact-driven source, however, it remained unclear what fraction of the Mg exosphere might be supplied from meteoric dust particles themselves and what fraction from Mg atoms released from the surface regolith. This motivated a search for correlations between UVVS and XRS measurements.

Because the production of Mg is greatest in the morning, we focused on UVVS observations made near equatorial dawn in our search for variations that could be linked to XRS's surface Mg/Si map. A time series of line-of-sight Mg emission at dawn observed near 300-km tangent altitude between 11 July 2012 and 26 February 2015 (representing 11 Mercury years of data) is shown in Figure 1a. Because of the planet's highly eccentric orbit and close proximity to the Sun, the emission of Mg is seasonally dependent with a predominant emission peak near perihelion (Figure S2). Therefore, each peak in the Mg emission time series (Figure 1a) represents one Mercury year. Every other Mercury year is color-coded blue and red in Figure 1a, and it is clear that the years coded red peak with higher emission than the years coded blue.

Because of Mercury's 3:2 spin-orbit resonance, the same longitude on the surface is located at the dawn terminator every other Mercury year (Domingue et al., 2007). Thus, UVVS measurements occurred over the same geologic features every other year. As a result, an every-other-year enhancement as seen in Figure 1a could be related to regional composition variations in the surface.

To investigate if the every-other-year enhancement is correlated with the Mg-rich terrane, we mapped the near-equatorial location of the emission observations onto the XRS Mg/Si ratio map in Figure 1b, maintaining the blue and red color coding to denote every other Mercury year as in Figure 1a. The location of the points demonstrates that the latitude and longitude of the UVVS observations are repeatable and separated by 180° longitude in alternating years. There is a concentration of observations near 90°E and 270°E where the dawn

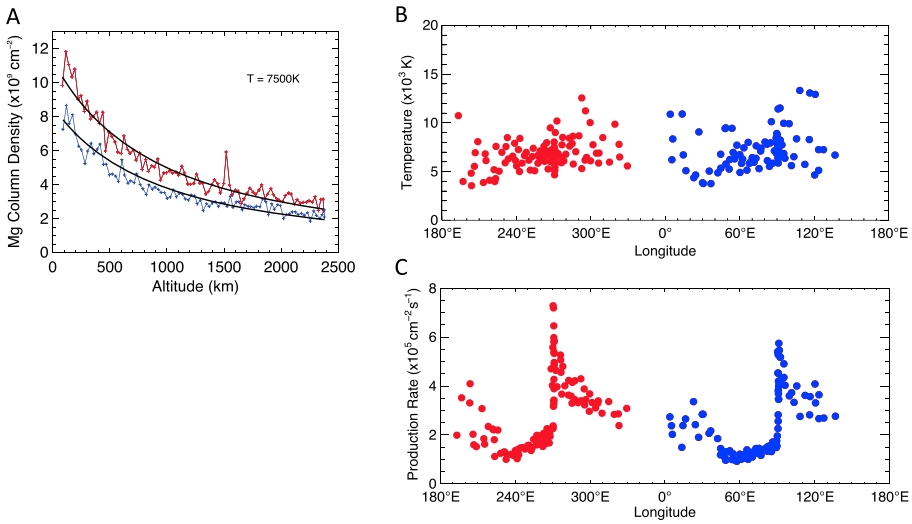

Figure 2. (a) Examples of Chamberlain model fits for two typical limb profiles at dawn. The red curve represents a limb profile taken near the equator at 270°E longitude and the blue curve represents a limb profile taken near the equator at 90°E longitude. The black curves represent the Chamberlain models that best fit each data set. (b) Characteristic temperature as a function of longitude. (c) Production rate as a function of longitude.

terminator spends half of its year near perihelion (Figure 3b). Figure 1c shows the corresponding emission versus longitude, indicating that there is a peak in emission over both sides of the planet (red and blue points). These two peaks show that the same seasonal variation occurs every year regardless of geographic location as illustrated in Figure 1a. However, the red points illustrate that the Mg emission is enhanced when observed over the Mg-rich terrane, confirming the first observed link between the exosphere and the regional composition of the surface.

The temperature of the released atoms provides clues about source processes. To investigate if the enhancement in exospheric Mg observed over the Mg-rich terrane originates from a different source process rather than simply from the terrane itself, we derived a characteristic temperature from the limb profiles (Figure S1). We assumed a Maxwellian velocity distribution and fit each dawn limb profile with the classic Chamberlain analytic model (Chamberlain, 1983; Chamberlain & Hunten, 1987). Merkel et al. (2017) applied a similar fitting analysis to seven Mercury years of UVVS dayside Mg limb profiles, covering local times from 6 a.m. to 6 p.m. Their analysis indicated that the bulk of exospheric Mg has a characteristic range of temperatures between 4000 and 8000 K, consistent with impact vaporization as the main driving source mechanism (either directly or through subsequent dissociation of a molecule). Although Merkel et al. (2017) did not rule out the possibility that sputtering contributes to the production of Mg, they determined that impact vaporization was the primary source in the equatorial region owing to the year-over-year regularity of the observations and the lack of any short-term temporal variations that would be expected from a highly variable source such as sputtering.

Figure 2a shows a comparison of a Chamberlain model fit to two different limb profiles—one observed over the Mg-rich terrane and one observed over the terrane on the other side of the planet. The red curve is a limb profile taken near the equator at 270°E longitude, and the blue curve represents a limb profile taken near the equator at 90°E longitude. Although the red curve indicates a higher Mg column density than the blue curve, the shapes of the two curves are the same, and the Chamberlain model fit returned the same temperature (7500 K), suggesting identical source processes. The higher column density in the red profile (over the Mg-rich terrane) is therefore an indication of a greater source rate due to more available surface Mg atoms and not from a different source process.

To confirm that the source process is the same for all data displayed in Figure 1, Figure 2b illustrates the characteristic temperature for all observations versus longitude. Although there is some scatter, the characteristic average temperature is the same across all terranes. A near-constant average temperature, regardless of geographic location, is further evidence that impact vaporization is the dominant source process for these two

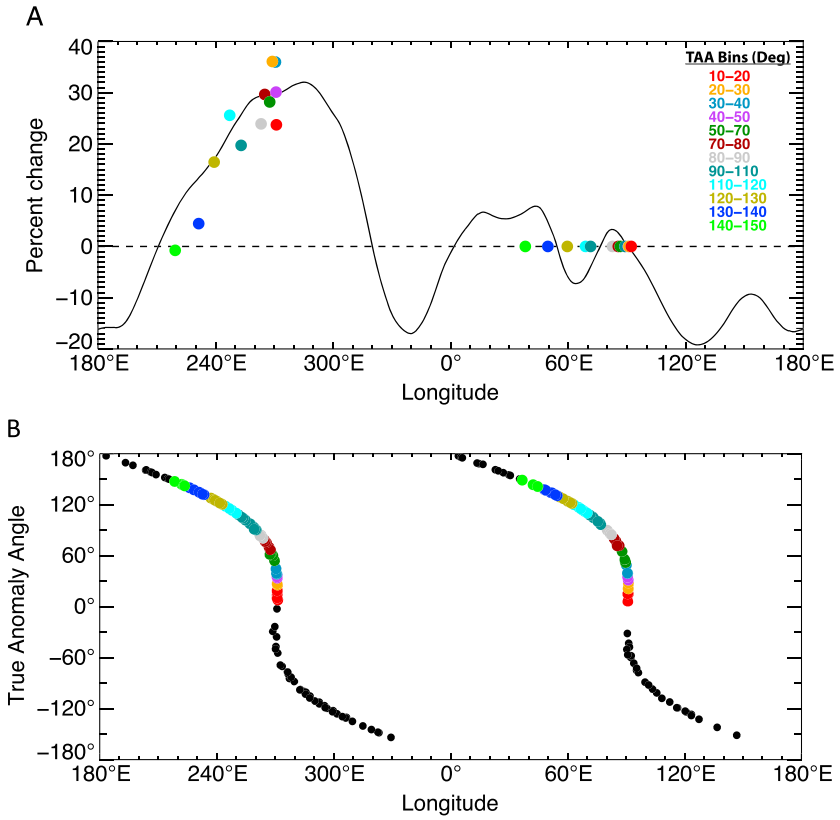

Figure 3. (a) Solid line represents the percent change of the equatorial slice through the XRS Mg/Si surface map (Figure 1b) relative to its value at 90°E longitude. Symbols represent the percent change of the equatorial (0° to −10° latitude) UVVS Mg production rate. The symbols represent the average in ~10° TAA bins, with the bins color coded as shown in the legend. Each TAA bin near 90°E is set at as the baseline for its corresponding bin near 270°E (see text for a more thorough description of the figure). (b) Plot illustrating how the true anomaly angle varies with longitude for the dawn Mg emission observations shown in Figure 1 (also see Figure S4). The color-coded points correspond to the TAA bins that lie between 0° and −10° latitude specified in (a). TAA = true anomaly angle.

regions. This result confirms that the increased abundance of Mg above the Mg-rich terrane is the cause of the every-other-year enhancement and clearly shows that a portion of the Mg exosphere is sourced directly from the surface regolith through impacts.

The production rate of exospheric Mg is a function of both temperature and near-surface density, two quantities that are derived from the Chamberlain model fits and is shown in Figure 2c. Because the seasonal production of Mg is influenced by its *g* value (the product of the efficiency rate by which Mg atoms scatter solar photons and the solar flux at the scattering wavelength; Killen et al., 2009), which is highly asymmetric about perihelion (Figure S3), the shape of the production rate curve with respect to longitude is different than that of the emission curve (Figure 1c). Nonetheless, because the temperature is nearly constant as shown in Figure 2b, Figure 2c illustrates that the production rate (like emission) is enhanced when over the Mg-rich terrane, with the enhancement most obvious between longitudes 240° and 280°.

To quantify the contribution of the surface to the local exospheric Mg density, we directly compare observations made within the Mg-rich terrane boundary to corresponding observations made on the opposite side of the planet. Figure 3a compares the Mg production rate (symbols) with the XRS-derived surface Mg/Si ratio (solid line) as a function of longitude with both quantities expressed as percent change from baseline values near 90°E. The solid line represents an equatorial slice through the XRS Mg/Si surface ratio map shown in Figure 1b and shows that the surface Mg/Si ratio is enhanced by 30% near 270°E longitude relative to its baseline value near 90°E longitude. However, as shown in Figures 1c and 2c, the variation of exospheric Mg with respect to longitude is more complicated than the XRS surface variation, because the exosphere variations are a combination of both the nominal seasonal variations and

contributions from a varying surface composition. Figure S4 illustrates how Mercury's true anomaly angle (TAA), the measure of Mercury's angular position relative to perihelion (seasonality), is coupled with longitude. Note that the variation of TAA with longitude is systematic and is the same for alternating years, with TAA values following a similar path across the surface but 180° apart in longitude. Therefore, to isolate and quantify the direct influence from the surface on the exosphere, we must account for the normal seasonal changes in the production rate when calculating the surface-contributed change.

We accomplished this by selecting a narrow latitude band (0° to −10°) near the equator, in order to compare *red-year* UVVS observations between longitudes 220°E and 270°E (where most of the UVVS observations fall directly over the enhanced surface) with their corresponding *blue-year* observations 180° away between 40°E and 90°E longitude (see Figure 1b). Figure 3b (comparable to Figure S4) illustrates that the variation of TAA with longitude is systematic. We use this systematic geometry to remove the seasonal component from the UVVS observations by averaging the production rate in ~10° TAA bins. The bins are arranged in pairs 180° apart in longitude, one near 270°E and the other near 90°E. Each pair is identified by a different color in Figures 3a and 3b. We calculate the percent differences between pairs assuming that the bins near 90°E reflect only the nominal seasonal Mg production rate, whereas those near 270°E reflect the seasonal plus the enhancement from the surface (Figure 3a). Because the TAA bins are compared in pairs, the baseline value for each pair lies on the zero percent line. Comparing pairs in this way cancels out the seasonal component in each bin.

For example, the light green points in Figures 3a and 3b represent an average over TAAs 140°–150° corresponding to longitudes 220°E and 40°E in the alternate years. We set the average production rate at 40°E as the base point, zero percent difference with itself, and use the average value to calculate the percent change to the observations near 220°E. In this example, the TAA bin is located outside the Mg enhancement and therefore there is no enhancement relative to its baseline seasonal variability near 40°E. In comparison, the gray points represent an average over TAA angles 80°–90°, corresponding to longitudes 265°E and 85°E. The production rate is enhanced by 24% when over the surface enhanced terrane near 265°E, relative to its baseline seasonal value (85°E). This process ensures that the enhancements observed in percent change in Figure 3a are not due to the underlying seasonal variation.

The colored symbols in Figure 3a illustrate that the production of exospheric Mg is enhanced by ~30% near 270°E longitude relative to its baseline values near 90°E longitude, in quantitative agreement with the XRS measurements. Moreover, as the UVVS observations move outside the Mg-rich terrane boundary to the west, both production and the surface abundance decrease at a similar rate. These results clearly confirm a 1:1 correlation between the longitudinal variation in production rate and the distribution of Mg on the surface.

3. Conclusions

The discovery of a direct link between changes in the local exospheric density and the regional variations in Mercury's surface material provides strong evidence that the local regolith composition plays an important role in sourcing the Mg exosphere. The link shows that for exospheric Mg, a significant, if not dominant, component of its source is directly coupled to the local crustal composition, and this result supports theoretical and experimental arguments that impact vaporization is able to directly source material from the regolith of rocky, airless bodies (Leblanc & Johnson, 2010). Because exospheric Mg is detected over all terranes and not just within the bounds of the Mg-rich terrane, a global surface reservoir, such as is the case for Na (Cassidy et al., 2016; Leblanc & Johnson, 2010), could still play a role in sourcing some fraction of the overlying Mg exosphere. However, the year-to-year regularity and lack of short-term temporal variations argue that for the observations analyzed here, sputtering is not an important contributor (but could be at higher latitudes). Similarly, the persistence of the observations from 1 year to the next suggests that material from the impactors themselves is a small contributor to the Mg exosphere given that we could reasonably expect the composition of such impactors to vary.

Because both Mg and Ca are refractory species, comparisons between them should provide further insight into their specific source processes, particularly given the established connections of Ca to dust from comet 2P/Encke (Killen & Hahn, 2015). The investigation of the Ca exosphere's relationship to the regional surface composition, and the comparison between Mg and Ca, is the subject of a future paper.

The observed 1:1 correlation of the production of Mg with the regional distribution of the surface composition will inform future exospheric models on both the location of the source material and an estimate of the enhanced density. Furthermore, because of Mercury's close proximity to its Sun and environmental conditions, it is representative of a class of rocky Mercury-like exoplanets, whose existence is now believed to be more common than previously thought (Santerne et al., 2018). Mercury is therefore an excellent laboratory for understanding airless body processes in general and can provide insights into the workings of airless exoplanets in other solar systems. With a proven link that exospheric Mg is directly tied to the surface regolith composition, future observations of Mg in the exospheres of rocky Mercury-like exoplanets could enable investigation of the compositional variation of their surfaces (Mura et al., 2011).

Acknowledgments
The MESSENGER mission is supported by the NASA Discovery Program. A. W. Merkel was supported by the NASA MESSENGER mission to Mercury and by NASA Discovery Data Analysis grant NNX15AM20G. R. Vervack and R. Killen both acknowledge support from the MESSENGER Participating Scientist Program and NASA Discovery Data Analysis programs. Data from the MESSENGER mission are archived in the NASA Planetary Data System.

References

Berezhnoy, A. A. (2018). Chemistry of impact events on Mercury. *Icarus*, *300*, 210–222. https://doi.org/10.1016/j.icarus.2017.08.034

Bida, T. A., Killen, R. M., & Morgan, T. H. (2000). Discovery of calcium in Mercury's atmosphere. *Nature*, *404*(6774), 159–161. https://doi.org/10.1038/35004521

Burger, M. H., Killen, R. M., Vervack, R. J. Jr., Bradley, E. T., McClintock, W. E., Sarantos, M., et al. (2010). Monte Carlo modeling of sodium in Mercury's exosphere during the first two MESSENGER flybys. *Icarus*, *209*(1), 63–74. https://doi.org/10.1016/j.icarus.2010.05.007

Cassidy, T. A., McClintock, W. E., Killen, R. M., Sarantos, M., Merkel, A. W., Vervack, R. J. Jr., & Burger, M. H. (2016). A cold-pole enhancement in Mercury's sodium exosphere. *Geophysical Research Letters*, *43*, 11,121–11,128. https://doi.org/10.1002/2016GL071071

Chamberlain, J. W. (1983). Planetary coronae and atmospheric evaporation. *Planetary and Space Science*, *11*, 901–960. https://doi.org/10.1016/0032-0633(63)90122-3

Chamberlain, J. W., & Hunten, D. M. (1987). *Theory of planetary atmospheres: An introduction to their physics and chemistry*, *International Geophysics Series* (2nd ed., Vol. 36). Orlando, FL: Academic Press Inc.

Domingue, D. L., Koehn, P. L., Killen, R. M., Sprague, A. L., Sarantos, M., Cheng, A. F., et al. (2007). Mercury's atmosphere: A surface-bounded exosphere. *Space Science Reviews*, *131*(1-4), 161–186. https://doi.org/10.1007/s11214-007-9260-9

Killen, R. M. (2016). Pathways for energization of Ca and Mg in Mercury's exosphere. *Icarus*, *268*, 32–36. https://doi.org/10.1016/j.icarus.2015.12.035

Killen, R. M., Bida, T. A., & Morgan, T. H. (2005). The calcium exosphere of Mercury. *Icarus*, *173*(2), 300–311. https://doi.org/10.1016/j.icarus.2004.08.002

Killen, R. M., Cremonese, G., Lammer, H., Orsini, S., Potter, A. E., Sprague, A. L., et al. (2007). Processes that promote and deplete the exosphere of Mercury. *Space Science Reviews*, *132*(2-4), 433–509. https://doi.org/10.1007/s11214-007-9232-0

Killen, R. M., & Hahn, J. M. (2015). Impact vaporization as a possible source of Mercury's calcium exosphere. *Icarus*, *250*, 230–237. https://doi.org/10.1016/j.icarus.2014.11.035

Killen, R. M., Potter, A. E., Vervack, R. J. Jr., Bradley, E. T., McClintock, W. E., Anderson, C. M., & Burger, M. H. (2010). Observations of metallic species in Mercury's exosphere. *Icarus*, *209*(1), 75–87. https://doi.org/10.1016/j.icarus.2010.02.018

Killen, R. M., Shemansky, D. E., & Mouawad, N. (2009). Expected emission from Mercury's exospheric species, and their UV-visible signatures. *The Astrophysical Journal Supplement*, *181*(2), 351–359.

Leblanc, F., & Johnson, R. E. (2010). Mercury exosphere I. Global circulation model of its sodium component. *Icarus*, *209*(2), 280–300. https://doi.org/10.1016/j.icarus.2010.04.020

McClintock, W. E., & Lankton, M. R. (2007). The Mercury atmospheric and surface composition spectrometer for the MESSENGER mission. *Space Science Reviews*, *131*(1-4), 481–521. https://doi.org/10.1007/s11214-007-9264-5

McClintock, W. E., Vervack, R. J. Jr., Bradley, E. T., Killen, R. M., Mouawad, N., Sprague, A. L., et al. (2009). MESSENGER observations of Mercury's exosphere: Detection of magnesium and distribution of constituents. *Science*, *324*, 610–613. https://doi.org/10.1126/science.1172525

Merkel, A. W., Cassidy, T. A., Vervack, R. J. Jr., McClintock, W. E., Sarantos, M., Burger, M. H., & Killen, R. M. (2017). Seasonal variations of Mercury's magnesium dayside exosphere from MESSENGER observations. *Icarus*, *28*, 46–54. https://doi.org/10.1016/j.icarus.2016.08.032

Morgan, T. H., Zook, H. A., & Potter, A. E. (1988). Impact-driven supply of sodium and potassium to the atmosphere of Mercury. *Icarus*, *75*(1), 156–170. https://doi.org/10.1016/0019-1035(88)90134-0

Mura, A., Wurz, P., Schneider, J., Lammer, H., Grießmeier, J.-M., Khodachenko, M. L., et al. (2011). Comet-like tail-formation of exospheres of hot rocky exoplanets: Possible implications for CoRoT-7b. *Icarus*, *211*(1), 1–9. https://doi.org/10.1016/j.icarus.2010.08.015

Nittler, L. R., Frank, E. A., Weider, S. Z., Crapster-Pregont, E., Vorburger, A., Starr, R. D., & Solomon, S. C. (2016). Global major-element maps of Mercury updated from four years of MESSENGER X-ray observations. *Lunar Planet. Sci.*, *47*, Abstract 1237. Retreived from https://www.hou.usra.edu/meetings/lpsc2016/pdf/1237.pdf

Potter, A. E., Anderson, C. M., Killen, R. M., & Morgan, T. H. (2002). Ratio of sodium to potassium in the Mercury exosphere. *Journal of Geophysical Research*, *107*(E6), 5040. https://doi.org/10.1029/2000JE001493

Potter, A. E., & Morgan, T. H. (1986). Potassium in the atmosphere of Mercury. *Icarus*, *67*(2), 336–340. https://doi.org/10.1016/0019-1035(86)90113-2

Raines, J. M., DiBraccio, G. A., Cassidy, T. A., Delcourt, D. C., Fujimoto, M., Jia, X., et al. (2015). Plasma sources in planetary magnetospheres: Mercury. *Space Science Reviews*, *192*(1-4), 91–144. https://doi.org/10.1007/s11214-015-0193-4

Santerne, A., Brugger, B., Armstrong, D. J., Adibekyan, V., Lillo-Box, J., Gosselin, H., et al. (2018). An Earth-sized exoplanet with a Mercury-like composition. *Nature Astronomy*, *2*(5), 393–400. https://doi.org/10.1038/s41550-018-0420-5

Sarantos, M., Killen, R. M., McClintock, W. E., Bradley, E. T., Vervack, R. J. Jr., Benna, M., & Slavin, J. A. (2011). Limits to Mercury's magnesium exosphere from MESSENGER second flyby observations. *Planetary and Space Science*, *59*(15), 1992–2003. https://doi.org/10.1016/j.pss.2011.05.002

Schlemm, C. E. II, Starr, R. D., Ho, G. C., Bechtold, K. E., Hamilton, S. A., Boldt, J. D., et al. (2007). The X-Ray spectrometer on the MESSENGER spacecraft. *Space Science Reviews*, *131*, 393–415.

Schmidt, C. A. (2013). Monte Carlo modeling of north-south asymmetries in Mercury's sodium exosphere. *Journal of Geophysical Research (Space Physics)*, *118*, 4564–4571. https://doi.org/10.1002/jgra.50396

Sprague, A. L., Kozlowski, R. W. H., & Hunten, D. M. (1990). Caloris Basin—An enhanced source for potassium in Mercury's atmosphere. *Science*, *249*, 1140–1142. https://doi.org/10.1126/science.249.4973.1140

Valiev, R. R., Berezhnoy, A. A., Sidorenko, A. D., Merzlikin, B. S., & Cherepanov, V. N. (2017). Photolysis of metal oxides as a source of atoms in planetary exospheres. *Planetary and Space Science*, *145*, 38–48. https://doi.org/10.1016/j.pss.2017.07.011

Weider, S. Z., Nittler, L. R., Starr, R. D., Crapster-Pregont, E. J., Peplowski, P. N., Denevi, B. W., et al. (2015). Evidence for geochemical terranes on Mercury: Global mapping of major elements with MESSENGER's X-Ray Spectrometer. *Earth and Planetary Science Letters*, *416*, 109–120. https://doi.org/10.1016/j.epsl.2015.01.023

Wurz, P., Whitby, J. A., Rohner, U., Martin-Fernandez, J. A., Lammer, H., & Kolb, C. (2010). Self-consistent modeling of Mercury's exosphere by sputtering, micro-meteorite impact and photon-stimulated desorption. *Planetary and Space Science*, *58*, 1599–1616. https://doi.org/10.1016/j.pss.2010.08.003